Egyptian Geophysical Society
EGS Journal, Vol. 8, No. 1, 103-116 (2010)

SOIL/BEDROCK CHARACTERISATION AND ENGINEERING PARAMETERS CALCULATIONS FOR THE KANTO REGION, CENTRAL JAPAN

M.M.F. Shokry[(1)] and N. Hirata[(2)]

1- Department of Geophysics, Faculty of Science, Ain Shams University, Cairo, Egypt, 11566
2- Earthquake Prediction Research Centre, Earthquake Research Institute, Tokyo University, Japan

خصائص التربة/صخر الأساس وحساب المعاملات الهندسية لمنطقة الكانتو، بوسط اليابان.

الخلاصة: تم استخدام المعلومات المتاحة والخاصة بشبكتى رصد الزلازل (*K-NET and KiK-net*) وذلك من أجل عمل تقييم إقليمى لمنطقة الكانتو. ومن خلال هذه الدراسة تم عمل تقييم لمنطقة الدراسة من خلال دراسة الخصائص الهندسية والجيوتقنية لكل من طبقات التربة وصخر الأساس وذلك لخدمة الأهداف الهندسية. حيث تم حساب عدد من المعاملات الهندسية مثل معامل التركيز، معامل المادة، معدل تدرج الكثافة ونسبة التضاغط، وذلك من خلال الاستعانة بالمعلومات المتاحة والخاصة بشبكتى رصد الزلازل (K-NET and KiK-net) بالإضافة إلى أنه تم الاستعانة أيضا بعدد من تسجيلات الآبار الضحلة والعميقة والتى تصل إلى صخور القاعدة فى بعض الآبار. ولقد أظهرت نتائج المعاملات الهندسية التى تم حسابها والتى شملت قيم السرعات السيزمية ومعاملات الإنضغاط الهندسية توافقها مع النظام التركيبى الرسوبى السائد والمميز لمنطقة الكانتو. وأظهرت أيضا هذه الدراسة أهمية الاستفادة من المعلومات المتاحة والخاصة بشبكتى رصد الزلازل (*K-NET and KiK-net*) على موقع الإنترنت.

ABSTRACT: *Data from K-NET and KiK-net were used to evaluate regional site effects in the Kanto region. The present study delineates some of the shallow soil/bedrock engineering characteristics for construction purposes. A number of engineering parameters, such as Concentration Index Ci, Material Index γ, Density Gradient Di and Stress Ratio Si, were estimated using K- and KiK-NETS data together with shallow/deep borehole recordings obtained from the pre-Tertiary basement. Estimated parameters, which include seismic velocity values, engineering, consolidation and strength parameters showed that, these parameters are strongly correlated with the structure of the sedimentary layer-bedrock system in the Kanto region. The present study also delineates the usefulness of the K-NET and KiK-net data, which are now available on the internet site (www.k-net.bosai.go.jp/).*

INTRODUCTION

The Kanto region of Central Japan, which includes Tokyo, is located on Honshu, the largest island in Japan. The Kanto region is the centre of political and economic activities in Japan, and also contains one third of Japan's population. Its boundary is nearly the same as that of the Kanto plain. The region consists of seven prefectures: Gunma, Tochigi, Ibaraki, Saitama, Tokyo, Chiba and Kanagawa. It is one of the most active seismic zones in the world, and many disastrous earthquakes have occurred in and around the region. Due to the complex relative movement of the Philippine Sea, Pacific and the North American plates, complicated tectonic structures exist in this region, and several types of earthquake mechanisms have been observed (Okada and Kasahara, 1990; and Ishida, 1992). Recently, the metropolitan area has seen a large increase in the number of large-scale buildings, such as tall skyscrapers and large oil and gas tanks. The natural periods of these structures are long; thus they would be expected to respond to long-period ground motions determined by the sedimentary basin structure and the geophysical properties of bedrocks, basement rocks and sediments. More than 3000-meter thick sediments lie on the pre-Tertiary basement (the sedimentary section-basement system) beneath the Kanto region, similar in structure to many metropolitan areas throughout the world. Previous interpretations, based on geophysical exploration, suggest that the shape of the base of this sedimentary basin is smooth (Komazawa and Hasegawa, 1988; Koketsu and Higashi, 1992; Yamanaka and Yamada, 2002; and Suzuki, 2002) (Fig. 1).

Accurate evaluation of ground amplification characteristics requires detailed soil profile information, such as shear-wave velocity structures. It has been pointed out, however that, approximate estimation of ground amplification is possible with the shear-wave velocity of the surface layer (Borcherdt and Gibss, 1976) and that, the amplification of strong ground motion, such as peak ground velocity is correlated with the average shear-wave velocity from the surface to a certain depth (Joyner and Fumal, 1984; Midorikawa et al., 1994).

The ultimate goal of the present study is to recommend soil/bedrock characterisation and engineering parameters calculations for the Kanto region, based on the measured and calculated shallow engineering characteristics. Analysis of the down-hole seismic velocities (P-wave and S-wave) and density values could tangibly delineate the soil/bedrock layering in the study area, and also determine the following soil/bedrock engineering parameters: Poisson's Ratio, Young's Modulus, Lame's Constants, Concentration Index, Material Index, Density Gradient and Stress Ratio.

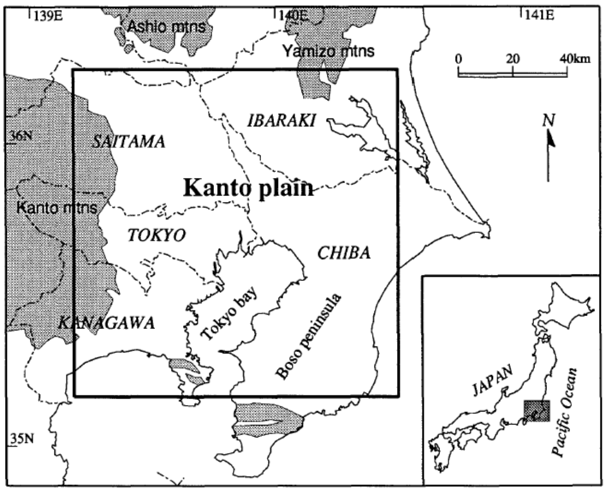

Fig. (1): Index map showing the location of the Kanto Region and its geographical and geological setting. The pre-Tertiary basement outcrops are shown in the shaded areas. The rectangle drawn with thick lines indicates the 120 × 120 km target area of the Kanto Region. The capital letters in italics designate the names of the prefectures in the Kanto Region.

To implement the engineering parameters calculations, data from systematic networks of strong-motion observation are needed. The National Research Institute for Earth Science and Disaster Prevention (NIED) constructed a strong-motion network, the K-NET (Kinoshita, 1998), followed by the construction of a high sensitivity digital strong-motion seismograph network (KiK-net) across all of Japan. The data from the K-NET and KiK-net are now available on the internet. In the present study, soil conditions information for the Kanto region were determined using K-NET and KiK-net sites data released on the internet.

DATA

The boundary between soil and bedrock is rarely distinct. It is usually gradual, making up a transition zone instead of a clear-cut interface. Residual soil (rock weathered or decomposed into a soil layer *in-situ*) is often encountered. When a residual soil layer is present in the transition zone, gravel, cobblestones and boulders may also exist, obscuring the location of the soil boundary. Below are few definitions of soil and rock taken from dictionaries of varying disciplines. The dictionary of Geological Definitions (Kulhawy et al., 1991) defines the term ‘soil’ as equivalent to regolith and ‘bedrock’ as any solid rock exposed at the surface of the earth or overlain by unconsolidated material. However, the Penguin Dictionary of Civil Engineering (Kulhawy et al., 1991) defines ‘soil’ as “gravels, sands, silts, clays, peat and all other loose materials including topsoil down to bedrock”, and ‘bedrock’ as “rock underlying gravel or other loose surface soil”. The representative values for shear-wave velocity possess through the following material classification limits: soft soil (less than 600 m/sec), firm soil (between 600 and 1800 m/sec), and rock (greater than 1800 m/sec) (Sjogren *et al.*, 1979). The last classification, the definition of which depends on the shear-wave velocity values, was used in the present study to differentiate between the sedimentary cover and the bedrock.

We used the down-hole soil conditions information from the K-NET and KiK-net station sites, which are well distributed in the Kanto region with a station-to-station distance of about 25 km. K-NET site data contain shallow down-hole soil conditions information (P-wave and S-wave velocities, as well as density values) for 110 stations. The down-hole measurements were obtained between depths of 10 to 20 m. At 33 stations, the borehole logs record the bedrock at various depths below the soil layer (sedimentary cover), but at the other 77 stations, bedrock is not recorded until the end of the borehole logs, while the sedimentary layer extends to the end depth of the borehole. However, KiK-net sites data contain deep down-hole soil measurements (P-wave and S-wave velocities) between about 100 to 2000 m in depth for 58 stations, that are well distributed in the Kanto region (Fig. 2).

ENGINEERING PARAMETERS

Elastic properties of the near-surface materials and their effects on seismic wave propagation are very important in earthquake and civil engineering, as well as in environmental and earth science studies. The increased amplitudes of soft sediments are one of the most important factors responsible for the amplification of earthquake motions. Amplification is proportional

$$\frac{1}{\sqrt{V_s.\rho}} \qquad (1)$$

where: (V_s) is the shear-wave velocity and (ρ) is the density of the investigated soil (Aki & Richards, 1980). No construction material has more variable engineering and physical parameters than the ground's soil. These parameters vary both laterally and vertically, and the variations are often robust (Bowles, 1982). In order to evaluate the competence of the subsurface for construction, some of the shallow soil engineering parameters were calculated. Four parameters were calculated; the Concentration Index (C_i), the Material Index (γ), the Density Gradient (D_i), and the Stress Ratio (S_i). Integration of these four parameters was used to classify the most appropriate areas of the Kanto region for construction.

Two types of units encountered in the Kanto region, identified on each lithologic column of the borehole logs and used from the K-NET and KiK-net sites, were the soil unit (sedimentary cover) and the bedrock unit. In order to calculate the above-mentioned parameters, the values of weighted mean values for V_p,

V_S and density (ρ) for the sedimentary cover and the bedrock were computed using the following formula:

$$V_p = \frac{\sum_{i=1}^{n} h_i}{\sum_{i=1}^{n} \frac{h_i}{V_{p_i}}} \qquad (2)$$

where: (h_i) and (V_{pi}) denote the thickness (in m) and the compressional wave velocity (in m/s) of the i-th layer in a total of n layers present in the same type of unit (Eurocode, 2001 and Romanian code, 2006). P and S-wave velocities and density were obtained from the acquired P-S logging data. When density data were lacking in some P-S logs, the following models relating density (in units of gm/c.c) and P-wave velocity (in km/sec) were applied: when V_p < 1.5 km/sec: ρ = 1.93 gm/cm^3 (Boore, 2007); if 1.5 km/sec $\leq V_p <$ 6.0 km/sec, then $\rho = 1.74 V_p^{0.25}$ (Gardner et at., 1974). Poisson's Ratio (σ), Young's Modulus (E), Lame's Constant (λ) and the Shear Modulus (μ) were also required. These elastic moduli values were calculated from the equations listed in Table 1.

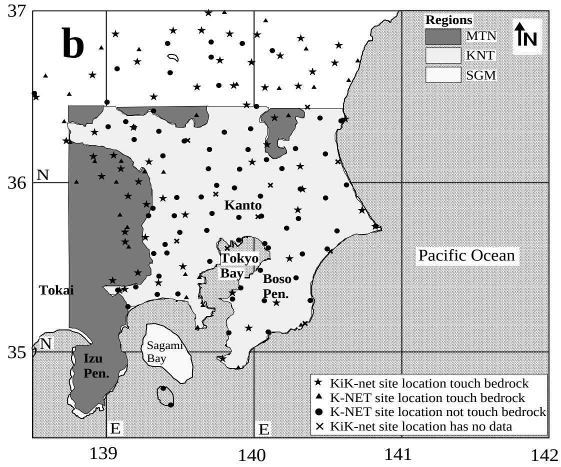

Fig. (2): a: Regional topographic map of Japan showing the finite difference (FD) grid area (black rectangle) of the Kanto district, including the Tokyo metropolitan area. Seafloor topography around Japan is also shown (Smith and Sandwell, 1997). b: Map showing the whole FD grid area and stations included in this study. Stars, triangles, circles, and crosses indicate the KiK-net site locations that reached bedrock, the K-NET site locations that reached bedrock, the K-NET site locations that did not reach bedrock, and the KiK-net site locations lacking data, respectively. The regions displayed in dark, medium, and light grey are the mountain region (MTN), the Kanto basin region (KNT), and the Sagami basin region (SGM) along the Sagami Trough, respectively. c: Geological map of the area surrounding the Kanto region reproduced from the Geological Survey of Japan (1992).

Table 1: List of equations used to calculate elastic moduli

Elastic Modulus	**Equation used**	**Reference**
Poisson's Ratio	$\sigma = \frac{1}{2}\left[1 - \frac{1}{(V_p/V_s)^2 - 1}\right]$	Adams (1951) and Salem (1990)
Young's Modulus	$E = \rho \frac{3V_p^2 - 4V_s^2}{(V_p/V_s)^2 - 1}$	Adams (1951)
Lame's Constants	$\lambda = \frac{\sigma E}{(1+\sigma)(1-2\sigma)}$	King (1966) and Toksoz et al. (1976)
Shear Modulus	$\mu = \frac{E}{2(1+\sigma)}$	King (1966) and Toksoz et al. (1976)
Elastic Modulus	Equation used	Reference
Poisson's Ratio	$\sigma = \frac{1}{2}\left[1 - \frac{1}{(V_p/V_s)^2 - 1}\right]$	Adams (1951) and Salem (1990)
Young's Modulus	$E = \rho \frac{3V_p^2 - 4V_s^2}{(V_p/V_s)^2 - 1}$	Adams (1951)
Lame's Constants	$\lambda = \frac{\sigma E}{(1+\sigma)(1-2\sigma)}$	King (1966) and Toksoz et al. (1976)
Shear Modulus	$\mu = \frac{E}{2(1+\sigma)}$	King (1966) and Toksoz et al. (1976)

V_P and V_S are the P- and S-wave velocities, respectively.

The elastic moduli results for the bedrock unit can be summarised as follows:

1. Soil cover thickness (depth to bedrock) ranged from 0.0 m (bedrock cropped out on the surface at station TKY002) to 250 m. Compared with the mountainous region (MTN) to the north and west, the central part of the Kanto basin region (KNT) is characterised by relatively thick soil cover (Fig. 3a). 2. Compressional wave velocity (V_p) is ranged from 650 to 4700 m/sec (Fig. 3b). 3. Shear wave velocity (V_s) is ranged from 255 to 2100 m/sec. The central part of the study area in the KNT region is characterised by relatively low shear-wave velocity values; these values increase toward the MTN region (Fig. 3c). Based on the shear-wave velocity, the bedrock is classified as firm soil (Sjogren *et al.*, 1979) in most parts of the study area, except in the KNT region, where it is classified as soft soil due to the low shear velocity values recorded. However, the geological description of the samples on the borehole logs refers to bedrock identification (Fig. 3d). 4. Bulk density (ρ) is ranged from 1.53 to 2.57 gm/cc. The area towards the northeast is characterised by relatively high rock densities. 5. Poisson's ratio (σ) is ranged from 0.083 to 0.495. 6. Young's modulus (E) is ranged from 333 to 31174 MPa (Mega Pascal = (Newton/m^2)/10^6). 7. Lame's constant (λ) is ranged from 160 to 34104 MPa. 8. Shear modulus (μ) or Rigidity modulus is ranged from 112 to 11334 MPa.

The northwestern and western parts of the area are characterised by relatively low Poisson's ratio values, indicating more competent soil in this part of the study area (Salem, 1990). The eastern part is characterised by relatively high values for Young's modulus, relatively low (λ) values, and relatively high rigidity or shear modulus (μ) values.

The elastic moduli results for the soil cover can be summarised as follows:

1. Compressional wave velocity (V_p) is ranged from 200 to 1900 m/sec (Fig. 4a). 2. Shear wave velocity (V_s) is ranged from 100 to 700 m/sec (Fig. 4b). The soil cover over the Kanto region is classified as soft soil, according to the shear-wave velocity (Sjogren *et al.*, 1979), excluding two sites (GNM015 and TCGH17), where the soil cover is classified as firm soil. 3. Bulk density (ρ) is ranged from 1.35 to 2.09 gm/cc (Fig. 4c). The area towards the central portion of KNT is characterised by relatively high soil densities. 4. Poisson's ratio (σ) is ranged from 0.24 to 0.5. 5. Young's modulus (E) is ranged from 43 to 2622 MPa. 6. Lame's constant (λ) is ranged from 39 to 6577 MPa. 7. Shear modulus (μ) or Rigidity modulus is ranged from 14 to 956 MPa.

The northwestern and western parts of the area are characterised by a relatively low Poisson's ratio, indicating more competent soil in this part of the study area. The central portion of KNT is characterised by relatively high values for Young's modulus, (E) values, and rigidity or shear modulus (μ) values.

At frequencies that approach the fundamental frequency (f_o) of the soil deposit, the transfer function began to take on large values. However, at frequencies above the fundamental frequency, a part of the soil deposits may be moving in one direction, while another part is moving in the opposite direction. The period of vibration corresponding to the fundamental frequency is termed the characteristic site period (T_s). T_s provides a very useful indication of the period of vibration, at which the most significant amplification can be expected. f_o and T_s were computed by using the following formulas: $f_o = (V_s/4H)$ and $T_s = (4H/V_s)$, respectively, where (V_s) is the shear-wave velocity and (H) is the soil cover thickness (Kramer, 2004). f_o is ranged from 0.38 to 32.5 Hz (Fig. 5a). T_s is ranged from 0.03 to 2.62 sec (Fig. 5b).

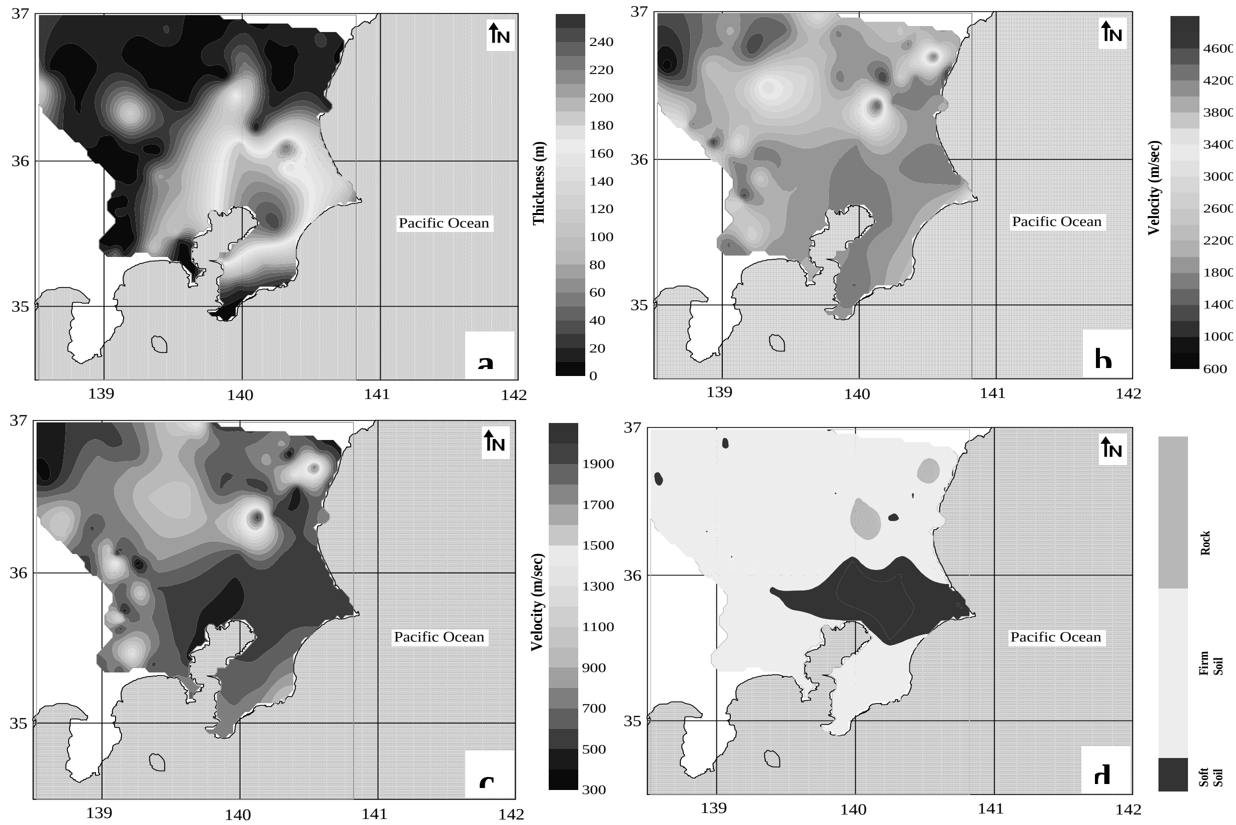

Fig. (3): a: Contour map illustrating the depth to the bedrock (sedimentary cover thickness). b: Contour map illustrating the compressional (P) wave velocity of the bedrock. c: Contour map illustrates the shear (s) wave velocity of the bedrock. d: Contour map illustrates the shear (s) wave velocity classification of the bedrock.

The area towards the central portion of KNT was characterised by relatively low f_o, which decreased as the soil cover thickness increased (Fig. 5c), but by relatively high T_s, corresponding to thick soil cover thickness with a nearly linear relationship (Fig. 5d). The results are consistent with those of Kinoshita and Ogue (2002), who found that high site amplification zones at low frequency bands of 0.5 and 1.0 Hz correspond to zones, in which the thickness of the soil layer exceeds 2.0 km, i.e., where the site amplification becomes large proportional to the thickness of the soil layer. At high frequency bands of 8 and 16 Hz, high site amplification zones correspond to mountainous areas; the Kanto mountains and high site amplification areas move from thick sediment zones to mountainous areas at frequency bands of 2.0 and 4.0 Hz.

Using the seismic velocities and elastic moduli values, the shallow soil/bedrock engineering parameters were calculated. These parameters include the Concentration Index, the Material Index, the Density Gradient, and the Stress Ratio.

The Concentration Index (C_i)

The Concentration Index is an engineering parameter, that indicates the degree of material concentration or impaction (competence) for foundation and other civil engineering purposes. It depends mainly on the elastic moduli of the materials and the depth-pressure distribution. Therefore, C_i is a material-dependent factor. Bowles (1982) formulated the concentration index in terms of Poisson's ratio (σ) as:

$$C_i = \frac{(1+\sigma)}{\sigma} \qquad (3)$$

Abd El-Rahman (1991) measured C_i in terms of velocities (P- and S-wave velocities, V_P and V_S) as:

$$C_i = \left(3-4\left\{\frac{V_s^2}{V_p^2}\right\}\right) / \left(1-2\left\{\frac{V_s^2}{V_p^2}\right\}\right) \qquad (4)$$

Abd El-Rahman (1989) summarised the ranges of the concentration index (C_i) corresponding to the degree of soil competence (Table 2). In the study area, the calculated (C_i) for the bedrock layer revealed values ranging from 3.02 to 12.99 (Fig. 6a). The northwestern part is characterised by relatively high (C_i) values, which according to Abd El-Rahman (1989), reflect fairly competent soft to good competent soil (Fig. 6b). For the soil cover, the calculated (C_i) displayed values ranging from 3.02 to 5.23 (Fig. 6c).

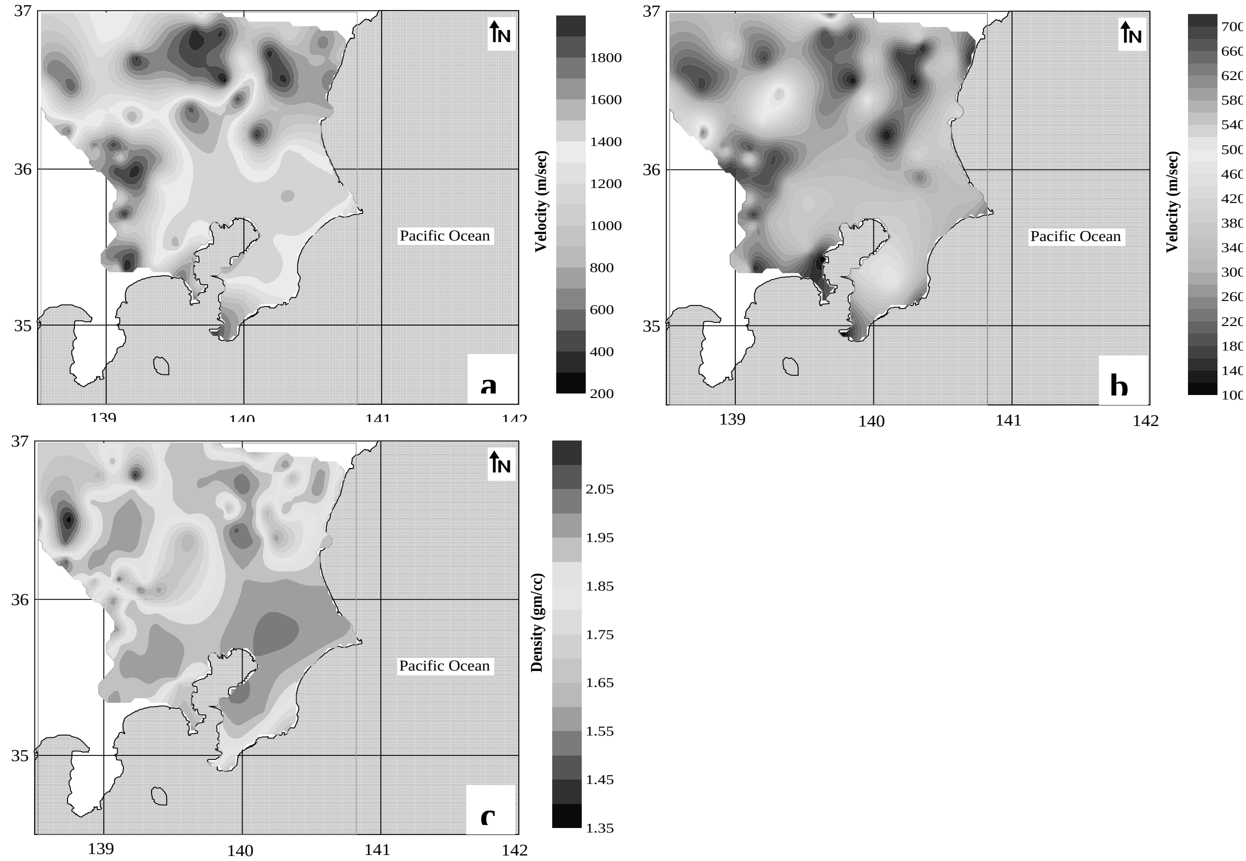

Fig. (4): a: Contour map illustrating the compressional (P) wave velocity of the sedimentary cover. b: Contour map illustrating the shear (s)-wave velocity of the sedimentary cover. c: Contour map illustrating the bulk density of the sedimentary cover. d: Gravity anomaly map reproduced from Kono and Furuse (1989). This anomaly map, includes the gravitational effects of subducting Philippine and Pacific slabs. The contour interval is 20 mgal.

The Kanto basin is characterised by relatively low (C_i) values, which classify this region as comprising non-competent, very soft soils to non-competent, soft soils toward the north-northwestern parts (Fig. 6d).

The Material Index (γ)

From the engineering viewpoint, the material index parameter defines the material quality for foundation purposes. According to Abd El-Rahman (1989), this expression addresses the degree of competence based on the elastic moduli of the given material. Thus, this index is associated with the composition of the material, the degree of consolidation, fracturing, jointing and the presence or absence of fluids in the pore space, all of which affect the medium of the materials and, consequently the wave velocities. Abd El-Rahman (1989) derived the material index from the ratio between Lame' s constant (λ) and the rigidity modulus (μ) or in terms of Poisson's ratio (σ) as follows:

$$\gamma = \frac{(\mu - \lambda)}{(\mu + \lambda)} = (1 - 4\sigma) \qquad (5)$$

According to Birch (1966), Gassman (1973), Tatham (1982) and Sheriff and Geldart (1986), Table 3 shows the Poisson's ratio, rigidity modulus and material index corresponding to various materials. For construction purposes, the soil properties can be classified by the material index into four main categories (Table 4). In the study area, the calculated material index (γ) for the bedrock layer revealed values ranging from -0.98 to 0.67 (Fig. 7a). The northwestern part was characterised by relatively high (γ) values, reflecting fairly to moderately competent material (Fig. 7b). For the soil cover, the calculated (γ) displayed values ranging from -0.98 to 0.06 (Fig. 7c). The Kanto basin is characterised by relatively low material index (γ) values, which are classified as non- to less-competent materials, but towards the north-northwestern parts, the material indices suggested that, the soils are fairly to moderately competent (Fig. 7d).

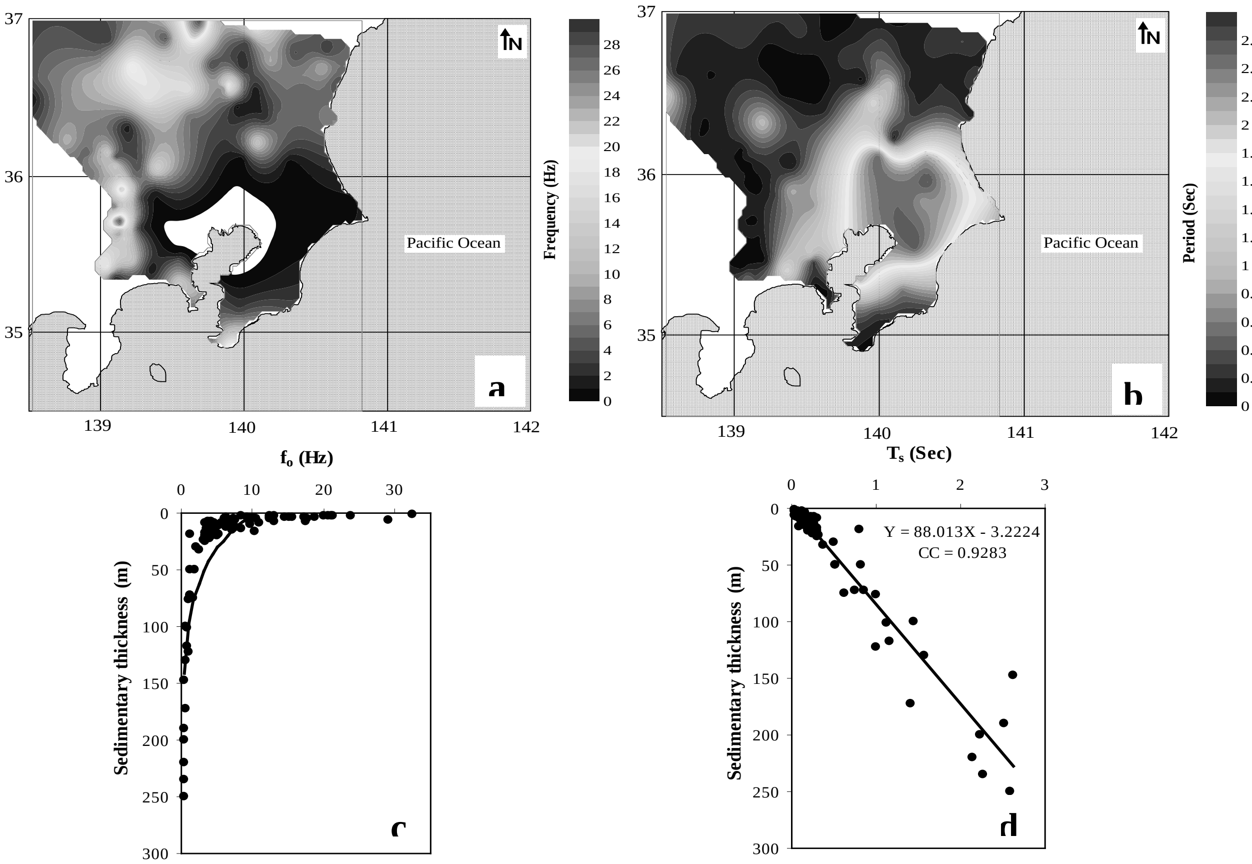

Fig. (5): a: Contour map illustrating the fundamental frequency (f_o) of the sedimentary cover. b: Contour map illustrating the characteristic site period (Ts) of the sedimentary cover. c: Relationship between the fundamental frequency (f_o) and the sedimentary thickness. d: Relationship between the characteristic site period (Ts) and the sedimentary thickness.

Density Gradient (D_i)

Adams (1951) introduced the quantitative form of the density gradient as:

$$D_i = \frac{\rho}{k} \tag{6}$$

where: (ρ) is the material density and (k) is the bulk modulus.

Stumpel *et al*. (1984) expressed the density gradient in terms of compressional and shear-wave velocities as:

$$D_i = \left(V_p^2 - \left[\frac{4}{3}\right] V_s^2 \right)^{-1} \tag{7}$$

In terms of the velocity-squared ratio (V_s^2/V_p^2), equation (7) can be written as:

$$V_p^2 D_i = \left(1 - (\frac{4}{3})(\frac{V_s^2}{V_p^2}) \right)^{-1} \tag{8}$$

Abd El-Rahman (1991) expressed this equation in terms of the velocity-squared ratio as:

$$D_i = (\frac{3}{V_p^2}) - \left(4(\frac{\mu}{E}) - 1 \right) = (\frac{3}{V_p^2}) - \left(\frac{(1-\sigma)}{(1+\sigma)} \right) \tag{9}$$

where: E is Young`s modulus.

Cordier (1985) summarised the ranges of ($D_i.V_{p2}$) corresponding to the degree of soil competence (Table 5). Equation (8) was used to calculate the density gradient ($D_i.V_{p2}$) for the bedrock unit in the study area. The calculated density gradient ($D_i.V_{p2}$) revealed values ranging from 1.01 to 2.54 (Fig. 8a). The northwestern area is characterised by relatively high ($D_i.V_{p2}$) values, reflecting moderately competent material (Fig. 8b). For the soil cover, the calculated ($D_i.V_{p2}$) displayed values ranging from 1.01 to 1.85 (Fig. 8c). MNT is characterised by relatively low ($D_i.V_{p2}$) values, which are classified as non-competent, very soft soil, although towards the north-northwestern parts, the materials classification is ranged from non-competent, soft soil to fairly competent soil (Fig. 8d).

Stress Ratio (Si)

During excess pressure caused by a stress change, consolidation settlement occurs. By the end of the consolidation process, the excess pressure is nearly zero

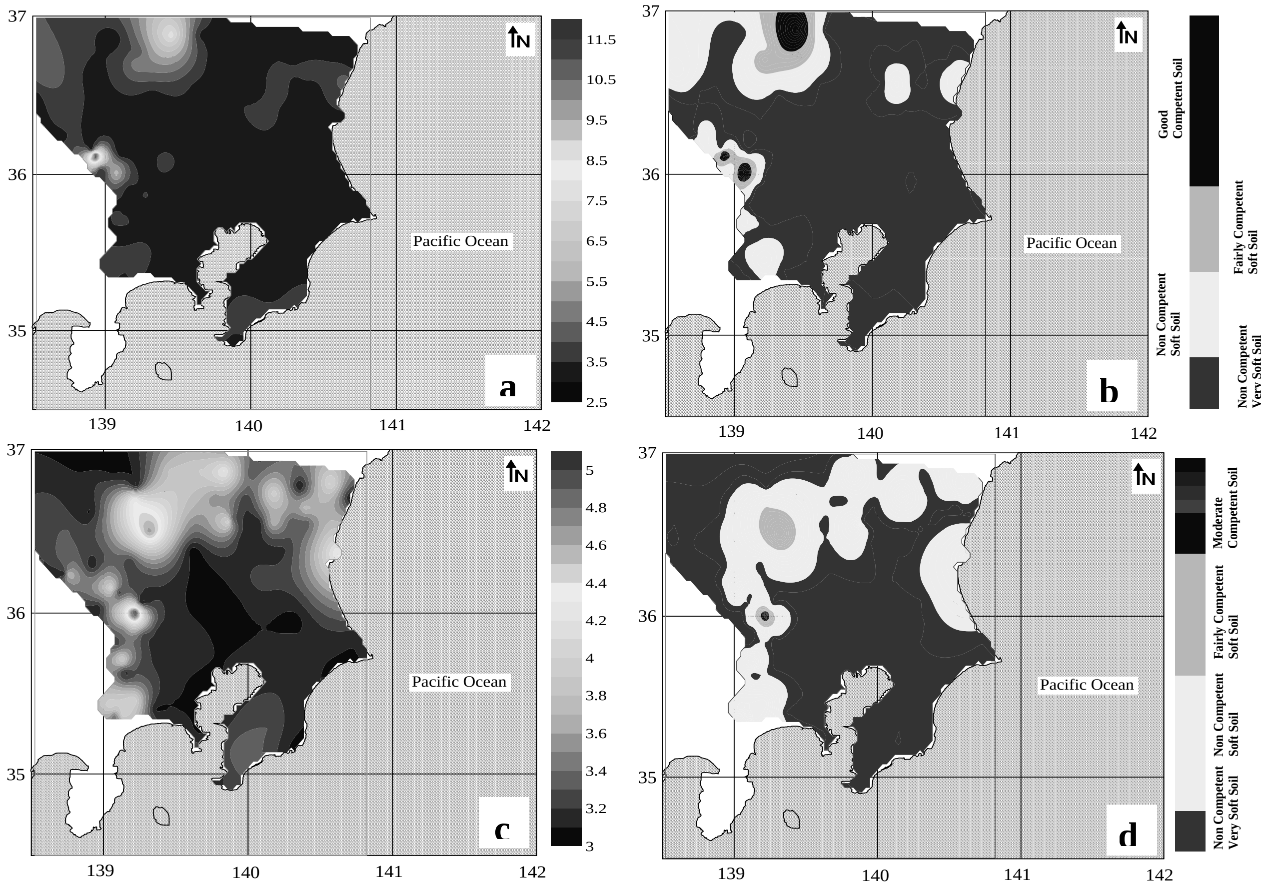

Fig. (6): a: Concentration Index lateral distribution for the bedrock. b: Concentration Index classification for the bedrock. c: Concentration Index lateral distribution for the sedimentary cover. d: Concentration Index classification for the sedimentary cover.

Table 2: Ranges of the concentration index and stress ratio that correspond to the soil competent degree, as described by Abd El-Rahman (1989).

	Weak		**Fair**		**Good**
	Incompetent		**Fairly competent**		**Competent**
	Very soft	**Soft**	**Fairly compacted**	**Moderately Compacted**	**Compacted**
Concentration Index C_i	3.5–4.0	4.0–4.5	4.5–5.0	5.0–5.5	5.5–6.0
Stress Ratio S_i	0.7–0.61	0.61–0.52	0.52–0.43	0.43–0.34	0.34–0.25

Table 3: Poisson's Ratio (σ), Rigidity (μ), and Material Index (γ) corresponding to different material, according to Birch (1966), Gassman (1973), Tatham (1982) and Sheriff and Geldart (1986).

Rock sample	**σ**	**μ**	**γ**
Liquids	0.5	0	-1
Perfect elastic rocks	0.25	$\mu = \lambda$	0
Very hard indurated rocks	0.00	$\lambda = 0$	+1

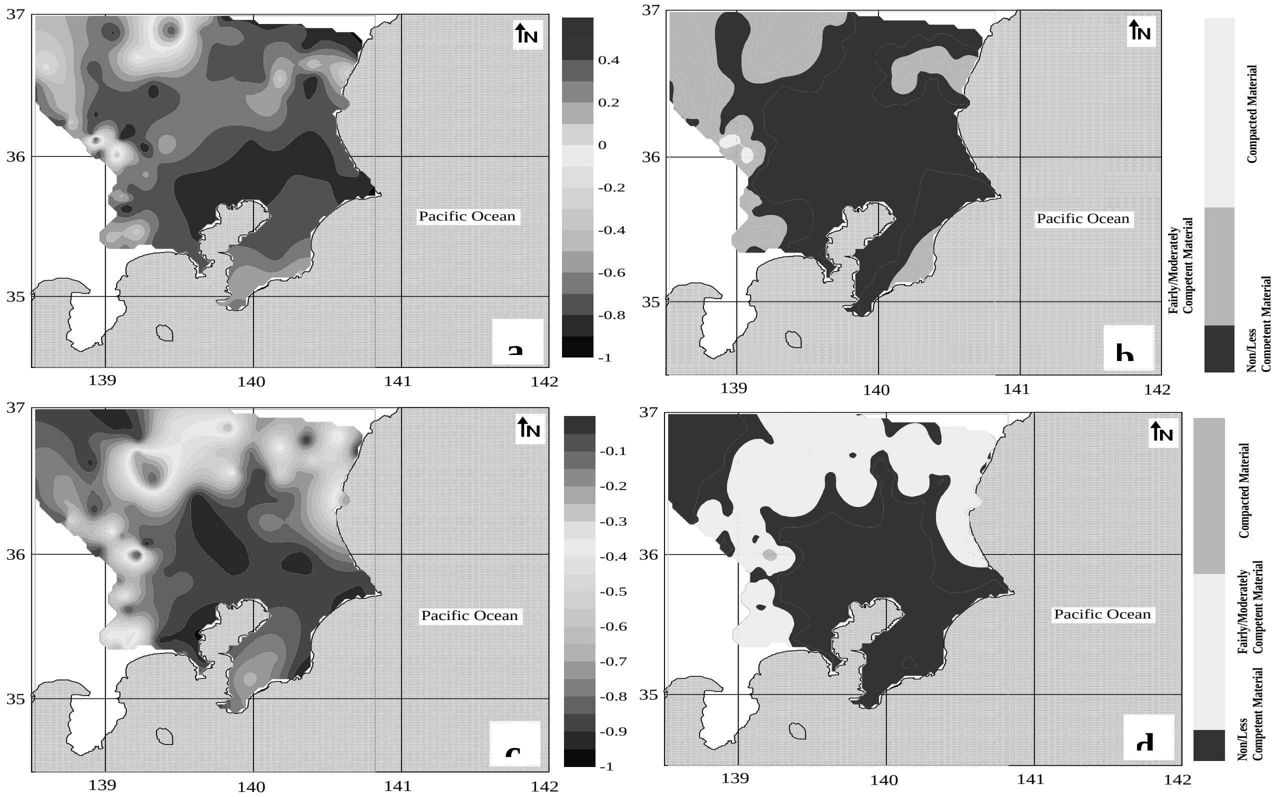

Fig. (7): a: Material Index lateral distribution for the bedrock. b: Material Index classification for the bedrock. c: Material Index lateral distribution for the sedimentary cover. d: Material Index classification for the sedimentary cover.

Table 4: Soil description with respect to Poisson's ratio and material index, as described by Birch (1966), Gassman (1973), Tatham (1982) and Sheriff and Geldart (1986)

Soil	**Incompetent**	**Fairly to**	**Competent**	**Very highly**
description	to slightly	moderately	materials	competent
parameters	Competent	Competent		materials
Poisson's Ratio σ	0.41-0.49	0.35-0.27	0.25-0.16	0.12-0.03
Material Index γ	(-0.5)-(-1)	(-0.5)-(0.0)	0.0-0.5	>0.5

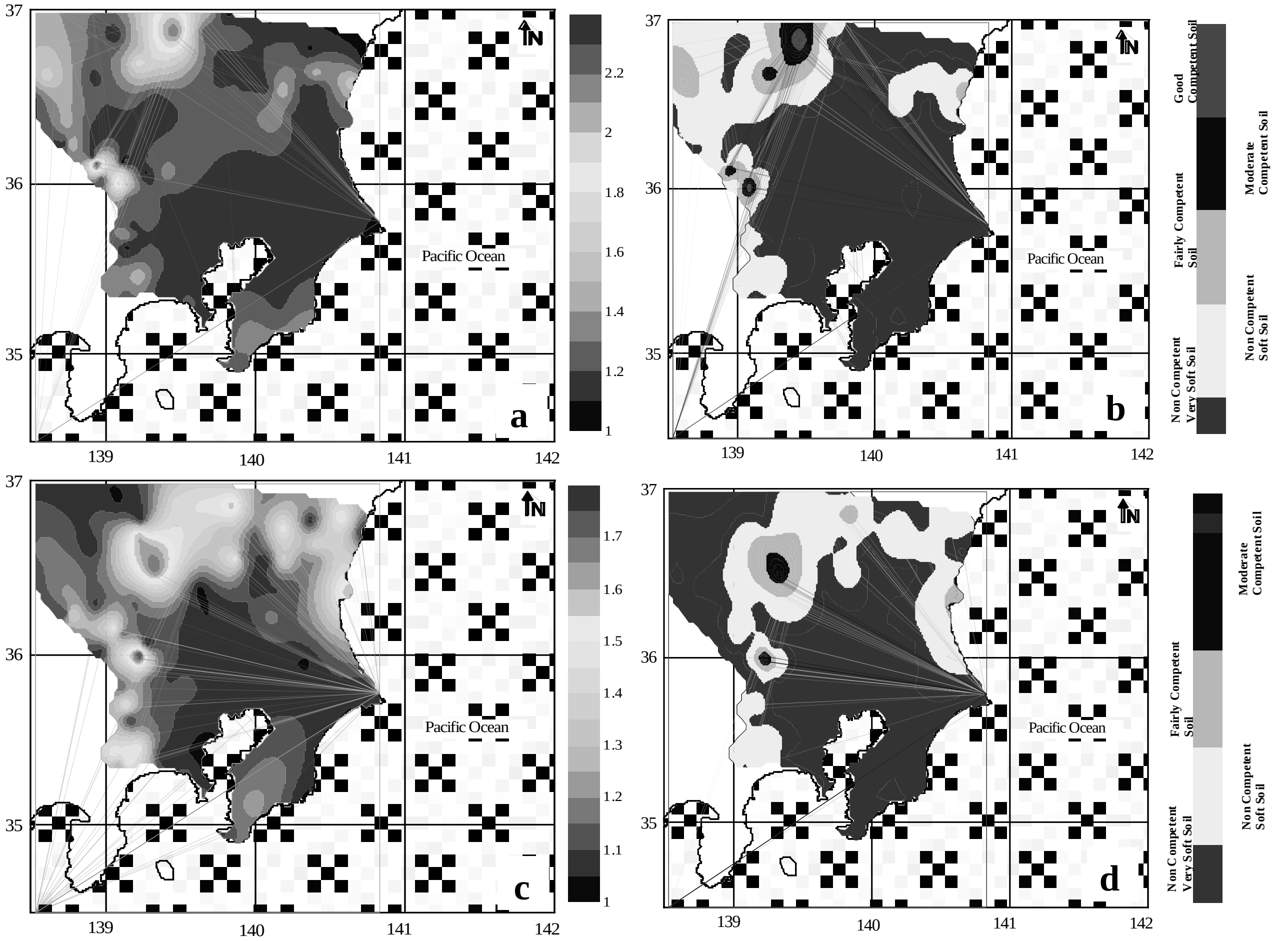

Fig. (8): a: Density Gradient ($D_i.V_{p2}$) lateral distribution for the bedrock. b: Density Gradient ($D_i.V_{p2}$) classification for the bedrock. c: Density Gradient ($D_i.V_{p2}$) lateral distribution for the sedimentary cover. d: Density Gradient ($D_i.V_{p2}$) classification for the sedimentary cover.

Table 5: Ranges of $D_i.V_{p2}$ corresponding to the degree of soil competence, according to Cordier (1985).

	Non competent		Fairly	Moderate	Good
	Very soft	**Soft**	**competent**	**competent**	**Competent**
$D_i.V_{p2}$	1.25–1.4	1.4–1.55	1.55–1.70	1.70–1.85	1.85–2.00

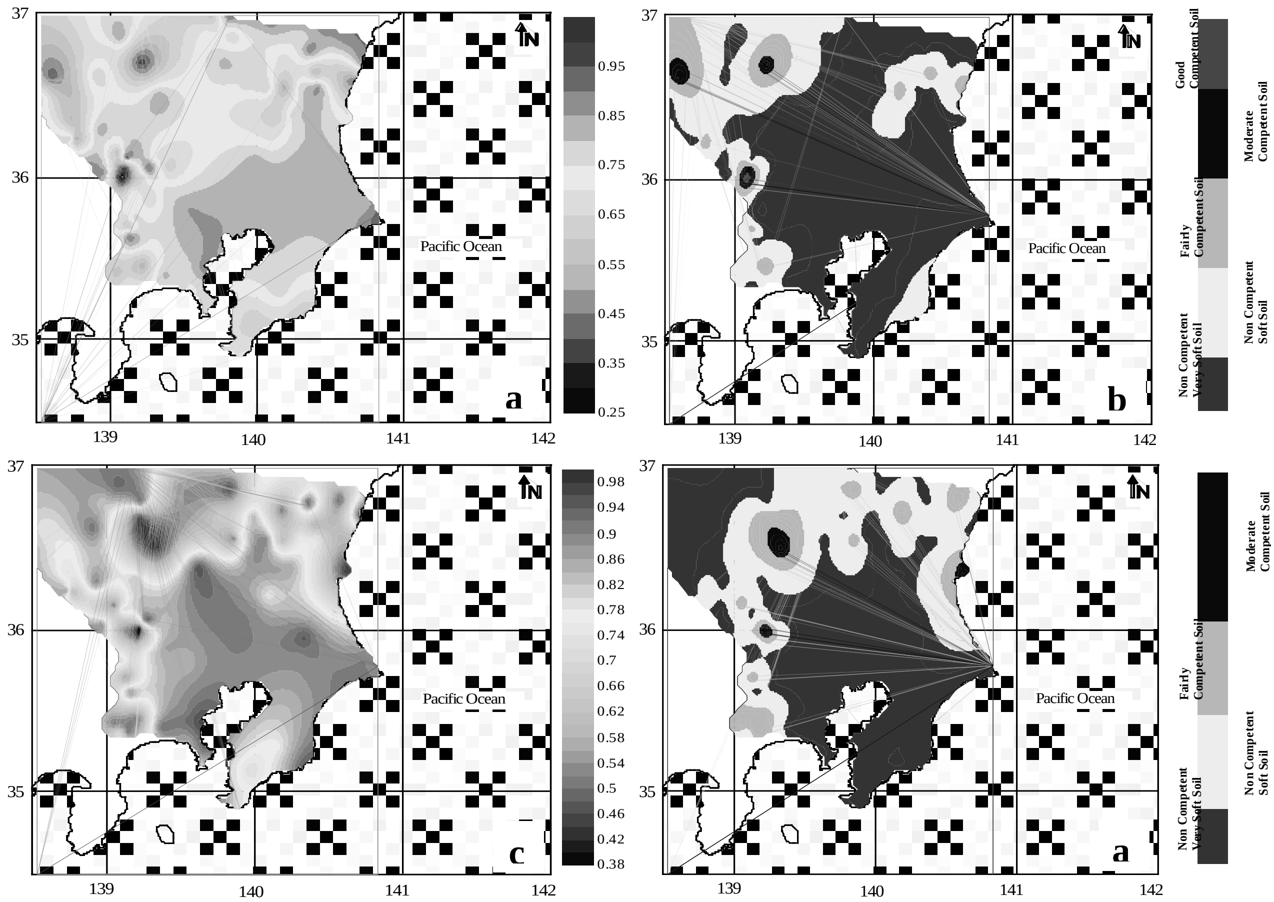

Fig. (9): a: Stress Ratio lateral distribution for the bedrock. b: Stress Ratio classification for the bedrock. c: Stress Ratio lateral distribution for the sedimentary cover. d: Stress Ratio classification for the sedimentary cover.

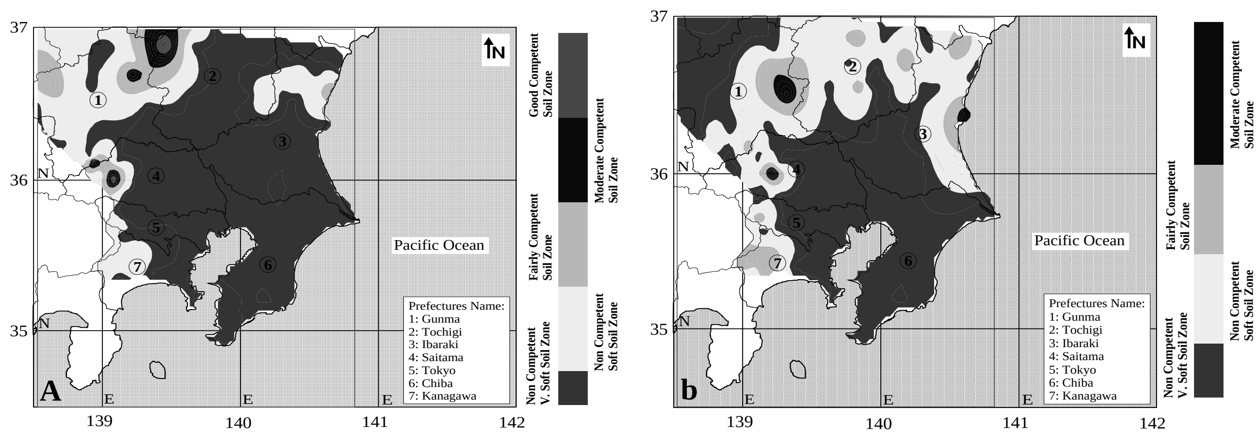

Fig. (10): a: Competence zones for the bedrock. b: Competence zones for the sedimentary cover.

and stress change will have changed from a total to an effective state. In this stress state, the soil state is defined as being in an equilibrium steady state condition of zero lateral and vertical strains (Bowles, 1982). Bowles (1982) pointed out that, there is a relationship between Poisson's ratio (σ) and stress ratio (S_i) for normally consolidated soils. This relationship was described by Bowles (1982) and Thomson (1986) as:

$$S_i = \frac{\sigma}{(1-\sigma)} \tag{10}$$

From several general observations about (S_i), Bowles (1982) pointed out that, S_i tends to be higher for fine soils than for coarse soils, that S_i is larger for loose cohesionless soils, that S_i tends to decrease with an increase in the overburden pressure, and that S_i is larger when the soil is over-consolidated. Abd El-Rahman (1991) pointed out the presence of a relationship between Poisson's ratio, S_i and P, S-wave velocities as:

$$S_i = 1-2(\frac{V_s^2}{V_p^2}) = (C_i - 1)^{-1} \tag{11}$$

Abd El-Rahman (1989) summarised the ranges of stress ratio (S_i) corresponding to soil competent degree (Table 2). In the study area, the calculated (S_i) for the bedrock layer revealed values ranging from 0.25 to 0.98 (Fig. 9a). The northwestern part is characterised by relatively high (S_i) values, which according to Abd El-Rahman (1989), reflect fairly competent to moderately competent soil (Fig. 9b). For the soil cover, the calculated (S_i) displayed values ranging from 0.31 to 0.98 (Fig. 9c). The Kanto basin is characterised by relatively low (S_i) values, which are classified as non-competent and very soft soil (Fig. 9d).

DISCUSSION

The study area is divided into zones according to the lateral variations in engineering parameters calculated for the bedrock and soil cover units (Fig. 10). The Kanto area is widely covered by Quaternary sediments at the Kanto basin, and this feature may affect the results obtained for the shallow layers. A geological map of the target region, reproduced from the Geological Survey of Japan (1992), is presented in Figure 1c. Although it is covered by Quaternary sediments due to the significant thickness of the sedimentary cover and deep depth of the bedrock in the Kanto basin (which includes the Ibaraki, Saitama, Tokyo, and Chiba prefectures), this area is classified as a non-competent and very soft soil zone (Fig. 10a). However, toward the north and northwest, the parts corresponding to mountainous areas (Fig. 1b & c) are classified as more competent, ranging from non-competent soft soil to moderately or good competent soil zones (Fig. 10b). Good correspondence is detected between the distribution zones with regard to the bedrock and soil cover units.

The gravity anomaly map in the study area, reproduced from Kono and Furuse (1989) (Fig. 4d), displayed low gravity anomalies in the Kanto basin (Boso Peninsula), as well as at the northwestern side towards the mountainous areas, and high gravity anomalies towards the northeastern side of the study area. Relatively good correspondence is observed in the bulk density distribution of the sedimentary cover in most of the areas, excluding some locations, such as the Boso Peninsula. Lack of correspondence in these areas may be related to the lack of log density data for the K-NET sites distributed in this area and to the empirical equations used to estimate the density values at the KiK-net sites, as well as to the interpolation process used to interpret the available density data (Fig. 4c).

CONCLUSION

This study proposes that, the K-NET and KiK-net are useful for evaluating the regional engineering parameters, yielding the following results:

(1) The engineering parameters evaluated are highly concordant with the soil layer/bedrock system in the Kanto region. These results are confirmed by comparing the geological data and those of other previous studies evaluating the pre-Tertiary basement.

(2) The Kanto basin, which includes the Ibaraki, Saitama, Tokyo and Chiba prefectures, is classified as a non-competent and very soft soil zone. However, toward the north and northwest, the parts corresponding to mountainous areas are classified as more competent zones, ranging from non-competent soft soil zones to moderately or good competent soil zones.

(3) To avoid the lack of necessary data for calculation of the engineering parameters, more borehole information are needed, according to the requirements of the engineering codes for geotechnical studies. Depending on the type of construction, these requirements include the number of drilled boreholes per constructed area, minimum spacing between the drilled boreholes, and the depth of the drilled boreholes.

REFERENCES

Adams, L.H., (1951): Elastic Properties of Materials of the Earth's Crust. Internal Construction of the Earth (edited by Gutenberg). Dover publications, Inc., New York.

Abd El-Rahman, M., (1989): Evaluation of the kinetic elastic moduli of the surface materials and application to engineering geologic maps at Maba-Risabah area (Dhamar Province), Northern Yemen. Egypt. J. Geol. 33 (1– 2), 229–250.

Abd El-Rahman, M., (1991): The potential of absorption coefficient and seismic quality factor in delineating less sound foundation materials in Jabal Shib Az Sahara area, Northwest of Sanaa, Yemen Arab Republic. Egypt, M. E. R. C. Earth Sci., vol. 5. Ain Shams University, pp. 181–187.

Aki, K., Richards, P.G., (1980): Quantitative Seismology. W. H. Freeman & Co., San Francisco.

Birch, F., (1966): Handbook of physical constants. Geol. Soc. Amer. Men. 97, 613.

Boore, D.M. (2007): Some thoughts on relating density to velocity, (http://quake.wr.usgs.gov/~boore/daves_notes/daves_notes_on_relating_density_to_velocity_v1.2.pdf).

Borcherdt, R.D., Gibss, J.F. (1976): Effects of local geological conditions in the San Francisco bay region on ground motions and the intensities of the 1906 earthquake, Bulletin of Seismological Society of America, Vol. 66, No. 2, pp.467-500.

Bowles, J.E., (1982): Foundation Analysis and Design, 2nd Ed. McGraw-Hill International Book Company, London, p. 587.

Cordier, J.P. (1985): Velocities in refraction seismology-Reidel Publishing Company Holland, 276 p.

EUROCODE-8-prEN1998-1-3, (2001): Design provisions for earthquake resistance of structures. European Committee for Standardisation.

Gardner, G.H.F., Gardner, L.W., Gregory, A.R., (1974): Formation velocity and density-the diagnostic basics for stratigraphic traps, Geophysics 39, 770–780.

Gassman, F., (1973): Seismische Prospektion. Birkhaeuser Verlag, Stuttgart, p. 417.

Geological Survey of Japan, (1992): Geological Atlas of Japan. Asakura Publishing, Tokyo, 2nd ed., 26 pp.

Ishida, M., (1992): Geometry and relative motion of the Philippine Sea plate and Pacific plate beneath the Kanto-Tokai district, Japan, J. Geophys. Res. **97**, 489–513.

Joyner, W.B., Fumal, T.E., (1984): Use of measured shear-wave velocity for predicting geologic and site effects on strong ground motion, Proc. 8th World Conference on Earthquake Engineering, Vol.2, pp.777-783.

King, T.V.V., (1966): Mapping organic contamination by detection of clay- organic processes. Proceeding AGWSE/NWWA/API.

Kinoshita, S., Kyoshin Net (K-NET), (1998): Seism. Res. Letters 69, 309-332.

Kinoshita, S., Ogue, Y., (2002): Site amplification of K-NET Sites in the Kanto Region, Central Japan. Seismotectonics in Convergent Plate Boundary, Eds. Y. Fujinawa and A. Yoshida, pp. 393-405.

Koketsu, K., Higashi, S., (1992): Three-dimensional topography of the sediment/basement interface in the Tokyo metropolitan area, central Japan. Bull. Seism. Soc. Am., **82**, 2328-2349

Komazawa, M., Hasegawa, I., (1988): The graben structure suggested by gravimetric basement in the Kanto district, central Japan. Mem.Geol. Soc. Japan, no. 31, 57-74.

Kono, Y., Furuse, N., (1989): Gravity anomaly map in and around the Japanese islands. Univ. Tokyo Press, Tokyo, 76 pp.

Kramer. S.L., (2004): Geotechnical Earthquake Engineering, 2nd Ed. Pearson Education (Singapore) Pte. Ltd., Indian Branch, p. 653.

Kulhawy, F.H., Trautmann, C.H., O'Rourke, T.D., (1991): The Soil-Rock Boundary: What Is It and Where Is It?, Geotechnical Special Publication No. 28: Detection of and Construction at the Soil/Rock Interface, pp. 1-15.

Midorikawa, S., Matsuoka, M., Sakugawa, K., (1994): Site effects on strong-motion records observed during the 1987 Chiba-ken-tohooki, Japan earthquake, Proc. 9th Japan Earthquake Engineering Symposium, Vol.3, pp.85-90.

Okada, Y., Kasahara, K., (1990): Earthquake of 1987, off Chiba, central Japan and possible triggering of eastern Tokyo earthquake of 1988, Tectonophysics 172, 351–364.

Romanian code for the seismic design for buildings, (2006): P100-1.

Salem, H.S., (1990): The theoretical and practical study of petrophysical, electric and elastic parameters o f sediments. Germany, Kiel Insitut for geophysik. Ph.D. thesis.

Sheriff, R.E., Geldart, L.P., (1986): Exploration Seismology. Cambridge Univ. Press,

Cambridge, p. 316.

Sjogren, B., Ofsthus, A., Sandberg, J. (1979): Seismic classification of rock mass qualities. Geophysical. Prospecting. 27: pp. 409-442.

Smith, W. H., Sandwell, D.T., (1997): Global sea floor topography from satellite altimetry and ship depth soundings, *Science* 277, issue 5334.

Stumpel, M., Kahler, S., Meissner, R., Nikereit, B., (1984): The use of seismic shear waves and compressional waves for lithological problems of shallow sediments. Geophys. Prospect. 32, 662–675.

Suzuki, H., (2002): Underground geological structure beneath the Kanto Plain, Japan. Rep. Nat. Res. Inst. Earth Sci. Disaster Prevention, no. 63, 1-19.

Tatham, R.H., (1982): Vp/Vs and lithology. Geophysics 47 (3), 336–344.

Toksoz, M.N., Cheng, C.H., Timur, A., (1976): Velocities of seismic waves-porous rocks. Geophysics **41**, 6 21–6 45.

Thomson, L., (1986): Weak elastic anisotropy. Geophysics 1954–1966.

Yamanaka, H., Yamada, N., (2002): Estimation of 3D S-wave velocity model of deep sedimentary layers in Kanto plain, Japan, using microtremor array measurements. Butsuri-Tansa, **55**, 53-65.